Neutron Diffraction Study of Structure I and Structure II Trimethylene Oxide Clathrate Deuterate

Adam J. Rondinone,*,† Bryan C. Chakoumakos,‡ Claudia J. Rawn,§ and Yoshinobu Ishii||

Chemical Sciences Division, Solid State Division, and Metals and Ceramics Division, Oak Ridge National Laboratory, Oak Ridge, Tennessee 37831 and Japan Atomic Energy Research Institute, Tokai, Ibaraki, Japan 319-1195

Received: October 3, 2002; In Final Form: March 27, 2003

Trimethylene oxide (TMO) forms structure I or II hydrates depending on stoichiometry and affords the opportunity to compare and contrast the temperature dependence of the crystal structure parameters for the two major hydrate structure types occluding a common guest molecule. Structures I and II TMO deuterates were synthesized from D_2O and hydrogenated TMO at the ratio of 6.25:1 D_2O:TMO (mole) for structure I and 17:1 D_2O:TMO for structure II. The samples were studied with powder neutron diffraction using the high-resolution powder diffractometer at the Japan Atomic Energy Research Institute, research reactor JRR-3M. The guest−host interactions of TMO in the $5^{12}6^2$ and $5^{12}6^4$ cavities were modeled using rigid-body constraints. Data were collected at 10 (12 K for structure I), 40, 70, 100, 130, 160, 190, 220, and 250 K for both structure types. The volumes of the 5^{12} and $5^{12}6^2$ or $5^{12}6^4$ cages of both structure types were computed at each temperature. Cage volume calculations, rigid-body orientations, and rigid-body mean-squared displacement parameters revealed perturbations in the host lattice due to guest molecule motion/orientation for the structure I deuterate but not for the structure II deuterate. The guest molecule motion approximates that in the gas phase with some restrictions imposed by the deuterate cage. Below 105 K, the guest molecule tends to orient the ether oxygen toward the hexagonal face of the structure I $5^{12}6^2$ cage. Above 105 K the ether oxygen moves away from the hexagonal face of the $5^{12}6^2$ cage to an angle of about 50°, corresponding to an increase in volume for the $5^{12}6^2$ cage and a decrease in volume for the 5^{12} cage. The most rapid changes with respect to temperature occur between 160 and 190 K. Similar behavior was not noted for the structure II deuterate.

Introduction

Trimethylene oxide (TMO) hydrate is of interest because it forms structure I or II hydrates depending on stoichiometry. The van der Waals radius of TMO is 6.1 Å, small enough to fit into structure I but also large enough to stabilize a structure II hydrate. In both structures the TMO molecule occupies only the larger ($5^{12}6^2$ or $5^{12}6^4$) cage.

Trimethylene oxide hydrate was first reported by Hawkins and Davidson,[1] who noted a dielectric relaxation similar to those for other structure II hydrates at one composition, but a different relaxation at a richer composition that they tentatively attributed to structure I. Sargent and Calvert[2] later verified the structure II crystal structure. Gough et al.[3,4] confirmed the structure I, reported a dielectric transition in the structure I hydrate at 105 K, and speculated that it was due to an ordering of the guest molecule ether group toward the hexagonal face of the $5^{12}6^2$ cage. Comper et al.[5] were not able to confirm this 105 K transition using adiabatic calorimetry, but they did report a structural change in the hydrate lattice at 169 K in the form of a sharp spike in the DSC data. Handa[6] reported calorimetric data that confirmed the presence of thermal anomalies at 107 and 168 K, but they suggested that the latter anomaly is due to a eutectic melt[7] rather than a structural transition.[5] Bertie and Jacobs[8] reported a possible interaction between the TMO guest molecule and the hydrate lattice at 100 K that was not seen in other hydrates. Detailed phase equilibria information was reported by Carbonnel and Rosso.[7,9] None of the above reports indicate such behavior in the structure II hydrate, in which the TMO molecule is less tightly confined. This study was undertaken in light of the aforementioned behavior of the structure I hydrate, to compare the two structure types under identical conditions with neutron powder diffraction, a technique well suited for studying materials composed of light elements.

Experimental Section

Deuterium oxide (CDN Isotopes, 99.9%) and TMO (Aldrich, 97%) were measured out gravimetrically in the proportions required (I, D_2O:TMO 6.25:1 mol; II, 17:1 D_2O:TMO). To prevent formation of structure II deuterate in the structure I sample,[3] the structure I sample was enriched slightly. Each solution was added dropwise, 1 drop/s, to a vanadium can suspended in liquid nitrogen. Each drop flash froze as it landed, reducing the effects of incongruent freezing. The cans were capped and placed into a freezer for 2 weeks for annealing at 240 K, close to their incongruent melting temperatures of 264 K (structure II) and 252 K (structure I) as reported by Rosso and Carbonnel.[7]

Neutron powder diffraction data were taken at 10 (12 K for structure I), 40, 70, 100, 130, 160, 190, 220, and 250 K at the high-resolution powder diffractometer (HRPD) at the Japan

† Chemical Sciences Division.
‡ Solid State Division.
§ Metals and Ceramics Division, Oak Ridge National Laboratory.
|| Japan Atomic Energy Research Institute.

10.1021/jp027127q CCC: $25.00
Published on Web 05/29/2003

Atomic Energy Research Institute, research reactor JRR-3M. The detector bank of the HRPD consists of 64 ^{3}He detectors. The experimental setup included a 6′ collimator before the detectors, a 12′ collimator before the Si (533) vertically focusing monochromator, and a monochromator takeoff angle of 89°. In this configuration the HRPD produced a monochromatic beam of neutrons with a 1.1635 Å wavelength that was calibrated using silicon powder. Data were collected with constant monitor counts with a step size of 0.05° over the 2θ range 5−160°. For temperature control, a closed-cycle He refrigerator equipped with two temperature sensors was used. Samples in sealed vanadium cans were removed from storage in N_2(l) and immediately attached to the precooled cold-tip of the refrigerator under a glovebag filled with He gas.

The diffraction patterns were analyzed using the general structure analysis system (GSAS).[10] Rigid-body constraints were used to approximate the orientational disorder of the TMO in the Rietveld refinements.[11] The atomic coordinates for both structure types have been reported previously.[12,13] The static picture of the dynamically rotating guest molecule can be visualized as spherical shells of nuclear density, generated by superimposing all the possible orientational configurations of the guest molecule centered within the cage. For the Rietveld refinement, this is achieved by defining a rigid-body molecule and placing that molecule into the cage at an angle so that each atom is in a general symmetry position. The space group symmetry of the crystal then operates on the molecule to generate several overlapping molecules that represent a range of possible orientations of the guest molecule within the cage. The occupancy of each site is adjusted according to the site multiplicity, so that the total nuclear density of each cage equals one molecule. The general positions in structure I have a multiplicity of 48, yielding 8 overlapping orientations in each $5^{12}6^2$ cage. The space group of structure II has a general site multiplicity of 192, yielding 24 overlapping orientations in each $5^{12}6^4$ cage. The starting angle of the guest molecule with respect to the site multiplicity is selected to produce the most homogeneous sphere of nuclear density. The starting angles are then allowed to refine and converge to an orientation that, when subject to the site symmetry, reflects some or all of the stable orientations of the guest molecule in the cage. Because TMO is polar, there is the possibility that the resulting distribution of nuclear density of the rigid body can be nonspherically symmetric; however, the minimum site symmetry of the large cages in structure I is tetragonal and in structure II is cubic.

Using rigid-body constraints, a single mean-squared displacement parameter (ADP) is refined for all the atoms in the molecule; that is, the atoms within the guest molecule experience thermal agitation and/or disorder in unison. Although there are interactions between the guest molecule and the deuterate framework,[14] the guest molecule is not bound ionically or covalently to the deuterate framework, and the displacements of the entire guest molecule are likely to dwarf the motion of each individual atom within the guest molecule. The ADPs of like atoms in each deuterate lattice were constrained to be the same in order to reduce the number of least-squares variables in the refinement. The GSAS TLS capabilities were initially employed, but in the course of the refinements only the translational parameters were allowed to isotropically refine; anisotropic variation as well as varying the rotational parameters caused unstable refinements.

Due to the incoherent scattering from the guest molecule, and the intrinsic disorder of the host framework and guest molecules, a radial distribution function was used to model the background. A flat background was first inserted into the refinement, and then the radial distribution coefficients were extracted from the Fourier transform of the raw data. The coefficients were inserted back into the radial distribution background function, and the relative weights of each coefficient were refined. Typically, the radial distribution coefficients were physically meaningful, in that they correspond to interatomic and intermolecular distances within the deuterate framework. Debye−Scherrer absorption corrections for a cylindrical sample were employed in the refinement. Calculated values of μ^*r were 1.74 for structure I and 0.79 for structure II.

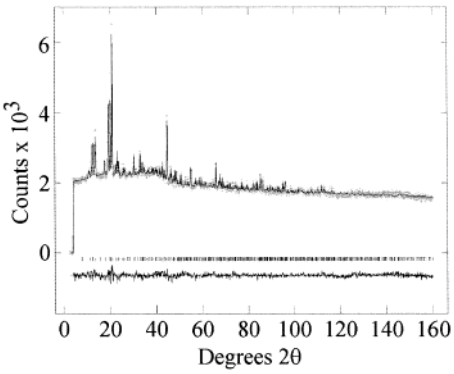

Figure 1. Rietveld refinement for structure I TMO deuterate neutron diffraction data collected at 12 K. No ice phase or structure II was present in this sample.

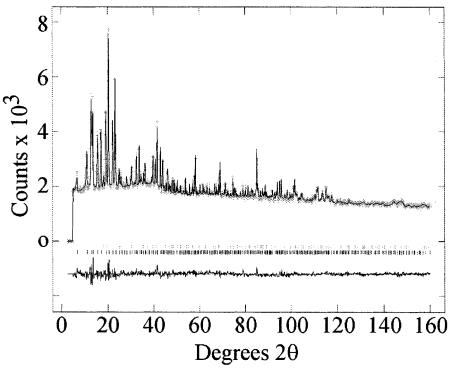

Figure 2. Rietveld refinement for structure II TMO deuterate neutron diffraction data collected at 10 K. A small (6.7 ± 0.01 wt %) fraction of ice was present and included in the refinement.

Results

Representative 10 and 12 K diffraction patterns are shown in Figures 1 and 2. The structure I deuterate (Figure 1) is free from ice, being made from a solution slightly rich in TMO. Structure II deuterate has a small (6.7 ± 0.01 wt %) fraction of ice present that was included in the Rietveld refinement as a second phase.

Tables 1 and 2 list atomic positions refined for the structure I and structure II data at 10 and 12 K. The reduced χ^2 for the structure I data listed in Table 1 is 1.312, and that for the structure II data listed in Table 2 is 1.839. Oxygen atoms are designated as O*i*, O*k*, and O*c*, and deuteriums are labeled D*ik* or D*ic* to represent their positions between the O*i*, O*k*, and O*c* oxygen atoms. Table 3 lists lattice parameters as a function of temperature. Although data were collected for the structure I deuterate at 250 K, the sample had begun to incongruently melt and the diffraction pattern was not usable. Above 100 K the thermal expansivity is linear up to the decomposition temper-

TABLE 1: Structure I Structure Data at 12 K[a]

	x	*y*	*z*	*f*[b]	U_{iso} (nm^2)
		Deuterate			
O*i*	0.1824(5)	0.1824(5)	0.1824(5)	1	2.17(7)
O*k*	0	0.3082(6)	0.1166(6)	1	2.17(7)
O*c*	0	1/2	1/4	1	2.17(7)
D*ck*	0.2316(9)	0.2316(9)	0.2316(9)	1/2	3.25(9)
D*ki*	0	0.4326(11)	0.1996(11)	1/2	3.25(9)
D*kk*	0	0.3765(12)	0.1547(12)	1/2	3.25(9)
D*ii*	0	0.3226(13)	−0.0365(10)	1/2	3.25(9)
D*kc*	0.0634(9)	0.2639(9)	0.1374(8)	1/2	3.25(9)
D*ik*	0.1181(8)	0.2286(9)	0.1643(11)	1/2	3.25(9)
		TMO Rigid Body			
O1	0.011(2)	0.306(1)	0.520(2)	1/8	3.17
C1	−0.084(2)	0.240(1)	0.502(2)	1/8	3.17
C2	−0.014(2)	0.137(1)	0.545(2)	1/8	3.17
C3	0.088(2)	0.219(2)	0.534(2)	1/8	3.17
H1	−0.159(2)	0.259(3)	0.552(3)	1/8	3.17
H2	−0.101(2)	0.229(1)	0.413(2)	1/8	3.17
H3	−0.034(2)	0.113(2)	0.631(2)	1/8	3.17
H4	−0.012(3)	0.065(1)	0.489(2)	1/8	3.17
H5	0.142(2)	0.222(2)	0.609(2)	1/8	3.17
H6	0.133(2)	0.201(3)	0.457(2)	1/8	3.17

[a] Space group = $Pm\bar{3}n$, a = 11.964 Å. [b] f = site occupancy.

TABLE 2: Structure II Structure Data at 10 K[a]

	x	*y*	*z*	*f*	U_{iso} (nm^2)
		Deuterate			
O*i*	0.1825(1)	0.1825(1)	0.3708(2)	1	1.45(3)
O*k*	0.2178(2)	0.2178(2)	0.2178(2)	1	1.45(3)
O*c*	1/8	1/8	1/8	1	1.45(3)
D*ii(a)*	−0.1618(3)	−0.0192(3)	0.1464(3)	1/2	2.19(4)
D*ii(b)*	0.1413(2)	.01413(2)	0.3733(5)	1/2	2.19(4)
D*ik*	0.1957(3)	0.1957(3)	0.3150(5)	1/2	2.19(4)
D*ki*	0.2050(4)	0.2050(4)	0.2729(4)	1/2	2.19(4)
D*kc*	0.1847(4)	0.1847(4)	0.1847(4)	1/2	2.19(4)
D*ck*	0.1591(3)	0.1591(3)	0.1591(3)	1/2	2.19(4)
		TMO Rigid Body			
O1	0.449(1)	0.347(2)	0.366(1)	1/24	1.22
C1	0.415(1)	0.415(2)	0.398(1)	1/24	1.22
C2	0.334(1)	0.369(1)	0.399(1)	1/24	1.22
C3	0.379(2)	0.308(1)	0.346(1)	1/24	1.22
H1	0.435(2)	0.433(2)	0.457(1)	1/24	1.22
H2	0.412(2)	0.462(2)	0.355(1)	1/24	1.22
H3	0.317(2)	0.347(2)	0.457(2)	1/24	1.22
H4	0.286(1)	0.400(2)	0.370(2)	1/24	1.22
H5	0.372(3)	0.247(1)	0.366(2)	1/24	1.22
H6	0.363(3)	0.317(2)	0.285(1)	1/24	1.22

ature for both structures with Pearson's coefficients of 0.998 and 0.999, respectively. The thermal expansivity for structure I between 100 and 220 K is 0.000 95 ± 0.000 03 Å/K. The thermal expansivity for structure II between 100 and 250 K is 0.000 81 ± 0.000 01 Å/K.

The positions of the oxygen atoms were used to calculate the volumes of each cage of each structure type using the program VINCI.[15] The results are plotted in Figures 3 and 4. The most interesting result is a clear decrease in volume for the structure I 5^{12} cage above 160 K. This corresponds to a reported anomaly in the thermal behavior,[5] as well as a sudden rise in volume for the $5^{12}6^2$ cage. Structure II showed only smooth increases in volume for both the small and large cages.

The displacement parameters of the oxygen, deuterium, and guest molecules of each structure type are shown in Figures 5 and 6. Figure 5 shows a steady increase in thermal motion with increasing temperature for the structures I and II deuterate framework. Figure 5a shows systematically higher values for atomic displacement parameters for structure I over structure II. The systematically higher values could be attributed to greater

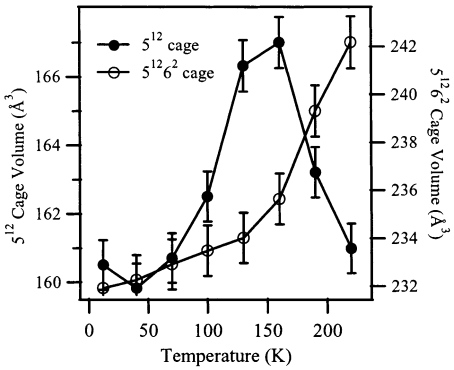

Figure 3. Structure I cage volumes. The larger, occupied cage volume increases steadily between 10 and 160 K and then at a faster rate between 160 and 220 K. The small unoccupied cage volume increases between 10 and 160 K and then decreases between 160 and 220 K. Error bars = ±3σ.

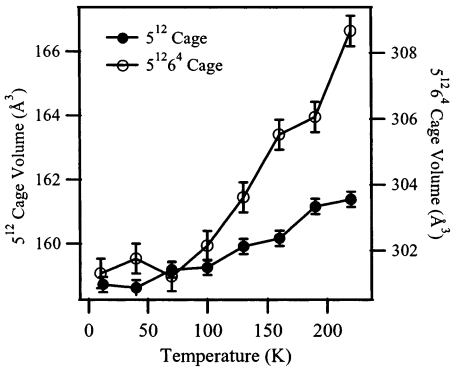

Figure 4. Structure II cage volumes. Structure II cage volumes increase proportional to increasing temperature. Error bars = ±3σ.

TABLE 3: Lattice Parameters

	a/Å	
T/K	structure I	structure II
str I: 12 K	11.964(1)	17.042(2)
str II: 10 K		
40	11.965(1)	17.045(1)
70	11.978(1)	17.051(1)
100	11.995(2)	17.061(1)
130	12.020(2)	17.086(1)
160	12.046(2)	17.108(2)
190	12.079(3)	17.131(2)
220	12.108(3)	17.158(1)
250		17.183(3)

disorder within the deuterate framework rather than increased thermal motion. Figure 6 shows the rigid-body displacement parameter for the guest molecule in each structure type.

The orientation angles of the guest molecule varied over the course of the refinements for the structure I deuterate. The angle between the C−O axis of the TMO molecule and the $\bar{4}$ axis of the $5^{12}6^2$ cage is plotted as δ in Figure 7. At low temperatures, the C−O axis of the guest molecule aligned with the $\bar{4}$ axis of the $5^{12}6^2$ cage (Figure 8a). Although shown as a single molecule for clarity, when operated on by the site symmetry, the structure I guest molecule would point both up and down with four replicates each turned by exactly 90°. These possible configurations represent the average orientation as the molecule moves. Above 100 K the C−O axis begins to decline from the 6^2 face (Figure 7) and then declines sharply by almost 60° between 160 and 190 K (Figure 8b). Structure II deuterate showed no such variation. The orientation of the guest molecule in structure

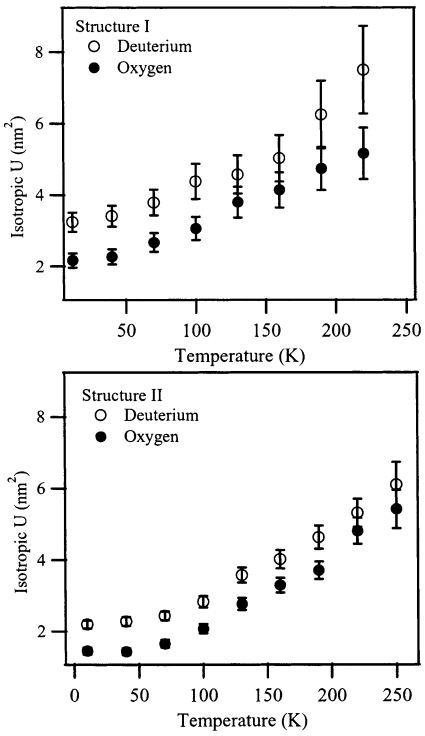

Figure 5. Mean-square displacement of the host lattice atoms in TMO deuterate structures I (a) and II (b). The zero-intercept for structure I is higher than that for structure II, suggesting greater disorder in structure I due to a tightly bound guest molecule. Error bars = $\pm 3\sigma$.

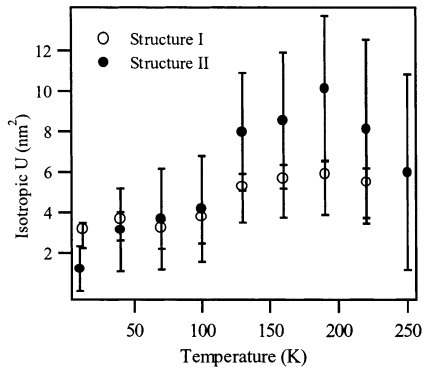

Figure 6. Mean-square displacement of the rigid-body guest molecule in TMO deuterate structures I and II. Error bars = $\pm 3\sigma$.

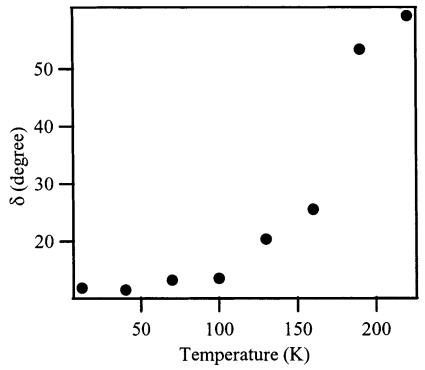

Figure 7. Angle δ between the C−O axis of TMO and the $\bar{4}$ axis of the $5^{12}6^2$ cage in structure I TMO deuterate.

II did not converge on any particular direction, so that when operated on by the site symmetry, a relatively homogeneous sphere of nuclear density was maintained (Figure 9).

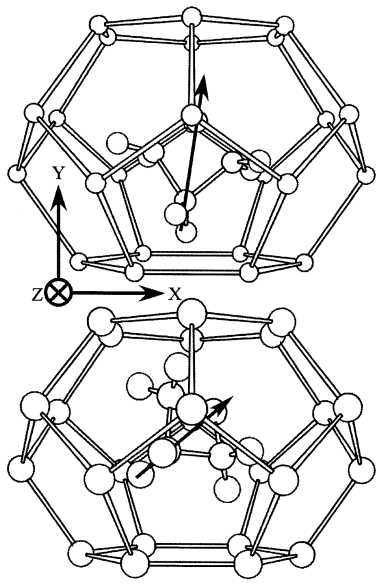

Figure 8. Reorientation of the guest molecule in the structure I $5^{12}6^2$ cage with increasing temperature. At 12 K (a, top), the ether group points toward the pentagonal face. At 220 K (b, bottom), the ether group has declined almost 60° from the $\bar{4}$ axis.

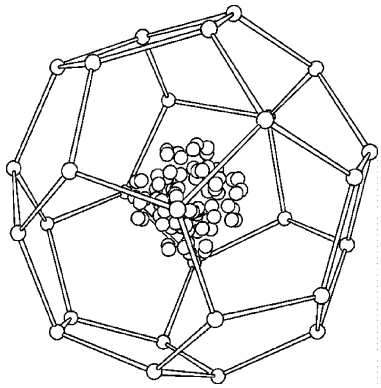

Figure 9. TMO deuterate structure II guest molecule with full symmetry shown. The multiplicity of each atomic site was adjusted so that the total nuclear density equals one molecule. The TMO guest molecule exhibits no orientational preference.

Discussion

The van der Waals diameter of the $5^{12}6^2$ cage of the structure I hydrate[3,5] is 0.58 nm, while the diameter of TMO across the carbon−oxygen axis[16] is 0.61 nm. For structure II,[2] the $5^{12}6^4$ cage diameter is 0.66 nm. The initial presumption for interpreting the cage volume trends is that for structure I the TMO molecule is tightly constricted into the cage and forces the cage to expand slightly to accommodate it.[3,17] Therefore, changes in the guest molecule motion or orientation are likely to be reflected in the cage volume or shape.

Figure 3 shows the structure I cage volumes with respect to temperature. Between 10 and 160 K the increase in volume for both types of cages (cage expansivity) is relatively constant with increasing temperature. At and above 160 K, the $5^{12}6^2$ cage expansivity increases. The change in the $5^{12}6^2$ cage expansivity is not reflected in the lattice expansivity, which remains constant above 100 K (Table 3). To compensate for the increase in $5^{12}6^2$ cage volume, which grows *relative* to the lattice constant, the smaller 5^{12} cage shrinks. Figure 3 shows that, at the same temperature that the $5^{12}6^2$ cage expansivity increases, the 5^{12} cage expansivity begins to decrease.

These trends are attributed to the movement or orientation

of the guest molecule. Previous studies that characterized the dielectric[3] and thermal properties[5] of structure I TMO hydrate reported on a guest molecule ordering transition at 105 K and a possible structural transition at 169 K. Gough et al.[3,4] argued that, below 105 K, dipolar guest−guest interactions dominate the behavior of the guest molecule and that dipolar chains form along adjacent $5^{12}6^2$ cages. The formation of the dipolar chain stabilizes the guest molecule from rapid dielectric relaxation and is, hence, responsible for the large decrease in permittivity reported. The current work confirms that the guest molecule moves toward the $\bar{4}$ axis between 130 and 100 K (Figure 7), which is consistent with chain formation. Although the current work cannot describe a dipolar chain formation due to symmetry limitations, in light of the previous results, a dipolar chain is certainly conceivable. Even if that is the case, a dipolar crystal is not possible because the chains lie along the ⟨100⟩ directions for the cubic symmetry of the crystal.

At higher temperatures between 160 and 190 K, the C−O axis of the guest molecule rapidly moves away from the $\bar{4}$ axis of the $5^{12}6^2$ cage according to the neutron refinements. This change coincides with the increase in $5^{12}6^2$ cage volume that begins at 160 K. This suggests that the guest molecule is capable of causing significant structural changes to the host lattice. Interestingly, the increase in cage volumes comes without an increase in the overall lattice parameter, as indicated by the constant expansivity of the lattice above 100 K, a situation reluctantly suggested by Bertie and Jacobs.[8] The extension of hydrogen bonds around the $5^{12}6^2$ cage and compression of hydrogen bonds around the 5^{12} cages is likely to have major implications on the spectroscopic data and could be useful in interpreting previously unexplainable results.[8]

While both structures I and II guest molecules exhibit a significant mean-squared displacement, the accompanying increase in cage volumes with increased temperature is only present in the structure I deuterate (Figure 9). The authors interpret this to be due to the greater volume of the larger $5^{12}6^4$ cage in structure II allowing more freedom of movement to the guest molecule and reducing the interactions between the guest molecule and the deuterate framework.

Furthermore, the structure II deuterate exhibits a systematically lower mean-squared displacement among the atoms in the deuterate framework, indicating that the framework is less structurally disordered. Future inelastic neutron scattering experiments will confirm if the systematically lower mean-squared displacement is due to thermal motion or disorder in the deuterate framework.

Conclusions

Crystallographic details for structure I and II TMO deuterate are presented over a broad temperature range. Structure I TMO deuterate exhibits structural transitions between 100 and 130 K, and again between 160 and 190 K, both attributed to a change in the guest molecule behavior. The change in behavior could be an additional degree of freedom representing rapid rotation and/or reorientation. The change in motion of the guest molecule causes an expansion of the $5^{12}6^2$ cage and constriction of the 5^{12} cage. These changes are not observed in the structure II TMO deuterate.

Acknowledgment. This research was sponsored in part by the Laboratory Directed Research and Development Program of Oak Ridge National Laboratory, managed by UT-Battelle, LLC for the U.S. Department of Energy under Contract No. DE-AC05-00OR22725. We acknowledge the support of the Japan Atomic Energy Research Institute.

References and Notes

(1) Hawkins, R. E.; Davidson, D. W. *J. Phys. Chem.* **1966**, *70*, 1889−1894.
(2) Sargent, D. F.; Calvert, L. D. *J. Phys. Chem.* **1966**, *70*, 2689−2691.
(3) Gough, S. R.; Garg, S. K.; Davidson, D. W. *Chem. Phys.* **1974**, *3*, 239−247.
(4) Davidson, D. W. In *Water: A Comprehensive Treatise*; Franks, F., Ed.; Plenum Press: New York, 1973; Vol. 2, pp 115−234.
(5) Comper, J.; Quesnel, A.; Fyfe, C.; Boyd, R. K. *Can. J. Chem.* **1982**, *61*, 92−96.
(6) Handa, Y. P. *Can. J. Chem.* **1985**, *63*, 68−70.
(7) Rosso, J.-C.; Carbonnel, L. *C. R. Acad. Sci.* **1972**, *C274*, 1108−1111.
(8) Bertie, J. E.; Jacobs, S. M. *J. Chem. Phys.* **1978**, *69*, 4105−4108.
(9) Carbonnel, L.; Rosso, J.-C. *J. Solid-State Chem.* **1973**, 304−311.
(10) Larson, A. C.; Von Dreele, R. B. General Structure Analysis System; Los Alamos National Laboratory: 1985.
(11) Swainson, I. Collaborative Computational Computation Project 14: http://www.ccp14.ac.uk, 2001.
(12) McMullan, R. K.; G. A. J. *J. Chem. Phys.* **1965**, *42*, 2725−2732.
(13) Mak, T. C. W.; McMullan, R. K. *J. Chem. Phys.* **1964**, *42*, 2732−2737.
(14) Klug, D. D.; Whalley, E. *Can. J. Chem.* **1973**, *51*, 4062−4071.
(15) Büeler, B.; Fukuda, K.; Enge, A. In *Polytopes—Combinatorics and Computation*; Ziegler, G. M., Ed.; Birkhäuser Verlag: Basel, 2000; Vol. 29.
(16) Dyadin, Y. A.; Zhurko, F. V.; Bondaryuk, I. V.; Zhurko, G. O. *J. Inclusion Phenom. Mol. Recognit. Chem.* **1991**, *19*, 39−56.
(17) Zele, S. R.; Lee, S.-Y.; Holder, G. D. *J. Phys. Chem. B* **1999**, *103*, 10250−10257.
(18) [a]Space group = *Fd*3*m*, *a* = 17.042 Å.